MEASUREMENT OF WIGNER DISTRIBUTION FUNCTION FOR BEAM CHARACTERIZATION OF FELs*

T. Mey#, B. Schäfer and K. Mann, Laser-Laboratorium e.V., Göttingen, Germany
B. Keitel, S. Kreis, M. Kuhlmann, E. Plönjes and K. Tiedtke, Deutsches Elektronen Synchrotron DESY, Hamburg, Germany

Abstract

Free-electron lasers deliver VUV and soft x-ray pulses with the highest brilliance available and high spatial coherence. Users of such facilities have high demands on phase and coherence properties of the beam, for instance when working with coherent diffractive imaging (CDI).
To gain highly resolved spatial coherence information, we have performed a caustic scan at BL2 of FLASH using the ellipsoidal beam line focusing mirror and a movable XUV sensitive CCD detector. This measurement allows for retrieving the Wigner distribution function, being the two-dimensional Fourier transform of the mutual intensity of the beam. Computing the reconstruction on a four-dimensional grid, this yields the Wigner distribution which describes the beam propagation completely. Hence, we are able to provide comprehensive information about spatial coherence properties of the FLASH beam including the mutual coherence function and the global degree of coherence. Additionally, we derive the beam propagation parameters such as Rayleigh length, waist diameter and the beam quality factor M².

INTRODUCTION

Operating a free-electron laser, detailed knowledge of its beam properties is required by users performing experiments as well as by beam scientists intending to maintain and improve the beam quality. Phase distribution and beam propagation factor M^2 can be retrieved by single shot wavefront measurements [1, 2]. A standard approach to gain information on the coherence properties of the beam is Young's double pinhole experiment [3]. Nevertheless, measuring the entire mutual coherence function $\Gamma(\vec{x},\vec{s})$ is an elaborate task since each single point $(\vec{x},\vec{s})$ in the four-dimensional phase space represents one experiment. For an adequate rasterization, quickly, this exceeds hundreds of thousands of shots.

We follow an alternate strategy to recover $\Gamma(\vec{x},\vec{s})$: measuring the Wigner distribution function (WDF) $h(\vec{x},\vec{u})$ offers access to the mutual coherence function since it is defined as the two-dimensional Fourier transform of the latter [4]. Similarly to measurements with UV lasers and synchrotron sources [5, 6] we have performed a caustic scan at BL2 of FLASH using the ellipsoidal beam line focusing mirror and a movable XUV sensitive CCD detector. For separable beams this is sufficient to completely map out the phase space of the Wigner distribution function [7]. The global degree of coherence is computed from $h(\vec{x},\vec{u})$ directly. A subsequent two-dimensional Fourier back-transform of the WDF yields the mutual coherence function and the coherence length of the beam is retrieved.

In this paper, we briefly summarize the theoretical background of the applied formalism and describe the experimental settings at FLASH. Subsequently, we present the resulting Wigner distribution and mutual coherence function together with the corresponding coherence parameters. Finally, we propose an extended experimental setup which offers an additional degree of freedom allowing an entire mapping of the phase space also for non-separable beams. First results carried out at this setup with several modes of an IR laser are presented proving the performance of the system.

THEORY

The Wigner distribution $h(\vec{x},\vec{u})$ of a quasi-monochromatic paraxial beam is defined in terms of the mutual intensity $\Gamma(\vec{x},\vec{s})$ as a two-dimensional Fourier transform of the latter [8]

$$h(\vec{x},\vec{u}) = \left(\frac{k}{2\pi}\right) \int \Gamma\left(\vec{x}-\frac{\vec{s}}{2},\vec{x}+\frac{\vec{s}}{2}\right) e^{ik\vec{u}\cdot\vec{s}} ds_x ds_y \qquad (1)$$

where $\vec{x}=(x,y)$ and $\vec{s}=(s_x,s_y)$ denote spatial and $\vec{u}=(u,v)$ angular coordinates in a plane perpendicular to the direction of beam propagation and k is the mean wave number of light. As Γ is Hermitian, h is real, although it may become negative in some regions. However, its marginal distributions with respect to $\vec{x}$ and $\vec{u}$ are always non-negative and yield the irradiance (near field) $I(\vec{x})$ and the radiant intensity (far field) $\hat{I}(\vec{u})$, respectively [9].

Propagation of the Wigner distribution through static and lossless paraxial systems, signified by a 4x4 optical ray propagation $ABCD$ matrix S from an input (index i) to an output (index o) plane writes [9, 10]

$$h_i(D\vec{x}-B\vec{u},-C\vec{x}+A\vec{u}) = h_o(\vec{x},\vec{u}). \qquad (2)$$

Likewise, the four-dimensional Fourier transform $\tilde{h}$ of h obeys a similar transformation law under propagation [10]

$$\tilde{h}_i\left(A^T\vec{w}+C^T\vec{t},B^T\vec{w}+D^T\vec{t}\right) = \tilde{h}_o(\vec{w},\vec{t}), \qquad (3)$$

where $(\vec{w},\vec{t})$ are the Fourier space coordinates corresponding to $(\vec{x},\vec{u})$. Considering a set $\{p\}$ of

*Work supported by Deutsche Forschungsgemeinschaft within Sonderforschungsbereich SFB755 "Nanoscale Photonic Imaging"
#tobias.mey@llg-ev.de

parameters and a set of irradiance profiles $I_{\{p\}}$ recorded at positions which are connected to an arbitrary reference plane via corresponding ray transformation matrices $S_{\{p\}}$, one obtains, according to the marginal property of h and well known Fourier relations

$$\int h_{\{p\}}(\vec{x},\vec{u})dudv = I_{\{p\}}(\vec{x})$$

$$\leftrightarrow \tilde{h}_{\{p\}}\left(\vec{w},\vec{t}=0\right) = \tilde{I}_{\{p\}}(\vec{w}) \qquad (4)$$

and from (3) and (4) [6]

$$\tilde{h}_{\text{ref}}\left(A_{\{p\}}^T\vec{w}, B_{\{p\}}^T\vec{w}\right) = \tilde{I}_{\{p\}}(\vec{w}). \qquad (5)$$

Propagation through free space in beam direction, i.e. in z-direction, is described by the $ABCD$ matrix

$$S_z = \begin{pmatrix} 1 & z \\ 0 & 1 \end{pmatrix} \qquad (6)$$

corresponding to the detector position z in the experimental arrangement described below. Thus, equation (4) becomes

$$\tilde{h}_{\text{ref}}(\vec{w}, z\cdot\vec{w}) = \tilde{I}_z(\vec{w}) \qquad (7)$$

representing a four-dimensional mapping relation between Fourier transformed intensity distributions and the Wigner distribution of the beam. Following this equation the phase space of $\tilde{h}$ is filled with data from intensity profiles measured at several positions z. A subsequent four-dimensional Fourier transform of $\tilde{h}$ results in the Wigner distribution function.

The global degree of coherence K is calculated by

$$K = \frac{\lambda^2}{P^2}\int h(\vec{x},\vec{u})^2\, dxdydudv\,. \qquad (8)$$

The mutual coherence function is derived by a two-dimensional Fourier back-transform

$$\Gamma(\vec{x},\vec{s}) = \int h(\vec{x},\vec{u})e^{-ik\vec{u}\cdot\vec{s}}dudv \qquad (9)$$

and the coherence lengths l_x and l_y are deduced as half width at half maximum of $\Gamma(0,0,s_x,0)$ and $\Gamma\left(0,0,0,s_y\right)$, respectively.

EXPERIMENTAL SETTINGS

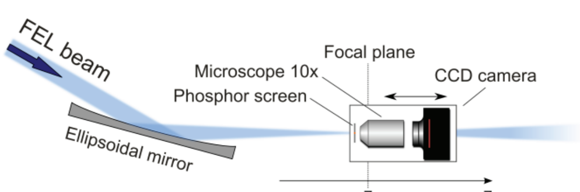

Figure 1: Experimental setup for caustic scan of the FLASH beam at BL2.

Figure 1 shows the experimental setup which has been employed for the caustic measurement of FLASH at BL2. Focusing is achieved by a carbon-coated ellipsoidal mirror with a focal length of 2m. The EUV sensor consists of a phosphorous screen (thickness ≈ 1µm) imaged onto a CCD chip by a 10x magnifying microscope. Resulting images have 1280x1024 pixels with an effective pixel width of 0.645µm resulting from the pixel size of the CCD of 6.45µm. A motorized translation stage allows for movement of the detector in z-direction within a range of 250mm, covering up to ten Rayleigh lengths $\bar{z}_R$ in both directions around the beam waist. During the caustic measurement, FLASH was running in single bunch mode with a charge of $Q = 0.3$nC at a wavelength of $\lambda = 19$nm. The beam energy was $E = 24$µJ and attenuation was accomplished by a 384.8nm thick meshless Nb-filter in order not to saturate the detector. An entire caustic of the beam was scanned within 48 minutes delivering 20 intensity distributions of single shots at each of 148 positions around the beam waist.

RESULTS

Beam profiles at four exemplary positions of the caustic of the FEL beam are displayed in figure 2 as measured in the experiment together with reconstructed profiles from the WDF which will be discussed later. Experimental data shows a strong modulation in x-direction while for y-direction the profiles are distributed much smoother. In the focal position ($z = 0$), the structure vanishes into a uniform distribution.

The evaluation starts with derivation of the standard beam propagation parameters such as Rayleigh length z_R, waist diameter d_0 and beam quality factor M^2 by a standard approach employing the second order beam moments [11]. Resulting beam parameters are summarized in table 1 unveiling relatively large M^2 values of 16 and 10 for x- and y-direction, respectively.

In order to visualize the computed Wigner distribution function we employ the projections $h_x(x,u) = \int h(\vec{x},\vec{u})dydv$ and $h_y(y,v) = \int h(\vec{x},\vec{u})dxdu$ which can be found in figure 3. In the (x,u)-plane h_x shows a streak structure while in the (y,v)-plane h_y is rather Gaussian-like. In that sense, $h(\vec{x},\vec{u})$ resembles the irregular horizontal radiating characteristic of FLASH which is already apparent in the beam profiles.

From the computed Wigner distribution function we reconstruct beam profiles at arbitrary positions z in the following fashion: $h(\vec{x},\vec{u})$ is propagated via equation (2) applying propagation matrix S_z from equation (6), subsequently the near field of the beam is generated by the integration $I_z(\vec{x}) = \int h_z(\vec{x},\vec{u})\, dudv$. The resulting intensity distributions are displayed in figure 2 below the corresponding beam profiles which have been captured experimentally. Apparently, a good agreement between measured and reconstructed profiles is achieved which confirms the validity of the obtained Wigner distribution.

ISBN 978-3-95450-126-7

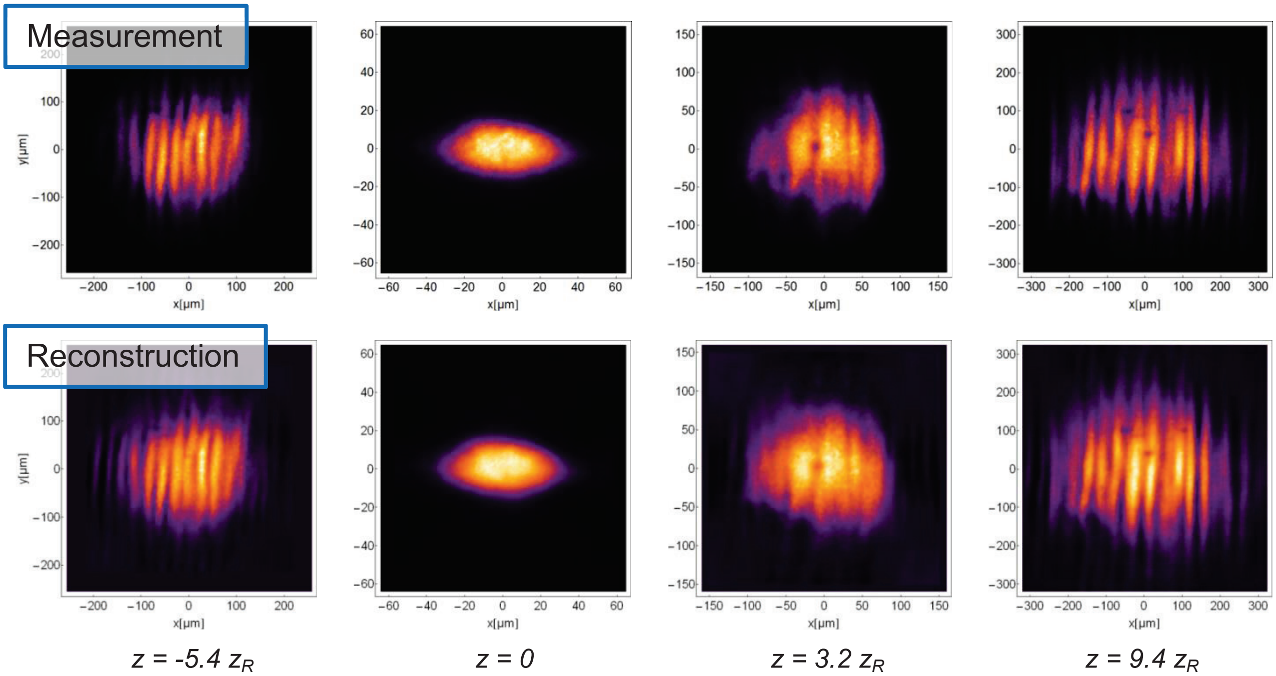

Figure 2: Normalized beam profiles at exemplary positions of the caustic. The upper row displays experimental data while the lower row shows reconstructed data from the Wigner distribution function.

Table 1: Beam Propagation Parameters and Coherence Parameters

	Waist diameter $d_0[\mu m]$	Rayleigh length $z_R[mm]$	Beam quality factor $M^2[1]$	Coherence length $l[\mu m]$	Global degree of coherence $K[1]$
x-direction	69	12.2	16	0.7	0.010
y-direction	32	4.3	10	1.1	

The mutual coherence function of the beam is reconstructed by application of equation (9). For illustration, the slices $\Gamma(x, 0, s_x, 0)$ and $\Gamma(0, y, 0, s_y)$ are employed and given in figure 4. Apparently, the shown distributions represent the beam diameter in x- and y-direction as expected while they decrease rapidly in s_x- and s_y-direction. This is quantified by the coherence lengths l_x and l_y (being derived as described in the theory section) which correspond to a small fraction of the beam diameter only. The exact values are given in table 1. The coherence for the vertical beam direction is found to be significantly larger than for horizontal direction.

The global degree of coherence is calculated as $K = 0.010$ unveiling an apparently low coherence of the FLASH beam.

In summary, the beam quality is determined to be comparatively better in vertical direction which is resembled by a more uniform corresponding Wigner distribution h_y, a lower beam propagation factor M_y^2 and a larger coherence length l_y.

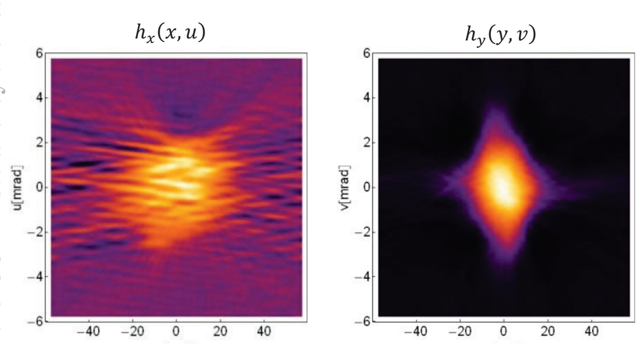

Figure 3: Projections of the Wigner distribution function.

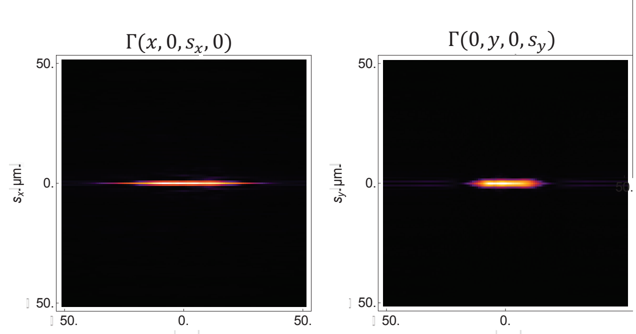

Figure 4: Slices of the mutual coherence function.

ISBN 978-3-95450-126-7

However, as compared to literature [3], our coherence parameters are lower by approximately one order of magnitude. We take two reasons into consideration:

- Our detector shows nonlinear behavior which effectively increases beam sizes and thus lowers coherence parameters. Investigation of this effect is part of a planned calibration measurement.

- With the present setup, for non-separable beams, we are able to measure three-dimensional sub-manifolds of h only, thus leaving gaps in its phase space which lower the value of K. This issue can be overcome by an extended experimental setup which is presented in the following outlook section.

OUTLOOK

In order to scan data which completely fills out the four-dimensional phase space of the Wigner distribution we propose an extended experimental setup as can be seen in figure 5.

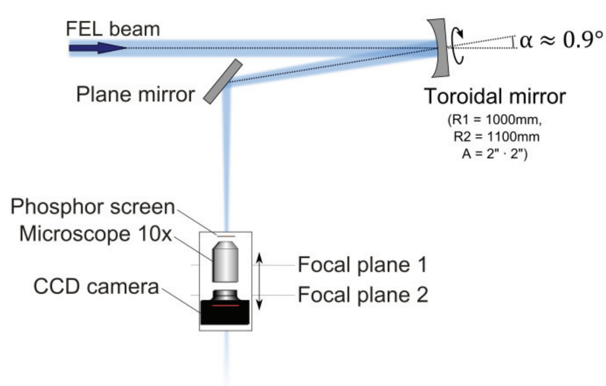

Figure 5: Extended experimental setup with toroidal mirror for four-dimensional phase space scanning.

The extended setup applies a rotatable toroidal multilayer mirror introducing a fourth degree of freedom into the system. Mathematically, this involves a more complex propagation matrix S which enables access to the entire phase space of the WDF. Thus, choosing measurement parameters in a proper way (rotation angles, camera positions), it is possible to reconstruct the entire Wigner distribution, also for non-separable beams.

First experiments have been carried out at a comparable test setup with an Nd:YAG laser in cw mode at a wavelength of 1064nm. Several modes (TEM00, TEM11, TEM20) were chosen by adjusting the resonator accordingly. In this case, a polished aluminum toroidal mirror with the radii 200mm and 300mm has been employed together with a standard CCD camera (1280x1024 pixels). Rotation of the mirror and movement of the camera has been achieved by servomotors. The automated measurement for each laser mode consists of 410 beam profiles in total, corresponding to 10 rotation angles and 41 z-positions. Exemplary results are given in table 2, displaying the radiation characteristics at the beam waist *before* the toroidal mirror. All distributions satisfy the expectations, though the near field of the TEM20 mode shows some artifacts in the outer regions. Since this beam is of a more complex structure, more profiles might be needed to sufficiently raster the phase space.

For all modes the computed global degree of coherence K matches the theoretical value K_{th} very well.

Further elaborate experiments with the introduced setup are planned for well-known visible and IR laser beams in order to characterize the performance of the system in more detail. In parallel we adopt the experiment for vacuum operation at FLASH working in the EUV range.

ACKNOWLEDGEMENTS

We kindly acknowledge support by Sonderforschungsbereich SFB 755 "Nanoscale Photonic Imaging" (project C8) from Deutsche Forschungsgemeinschaft.

REFERENCES

[1] B. Flöter et al., "EUV Hartmann sensor for wavefront measurements at the Free-electron LASer in Hamburg," New J. Phys. 12 (8), 083015 (2010).
[2] B. Flöter et al., "Beam parameters of FLASH beamline BL1 from Hartmann wavefront measurements," Nucl. Instr. and Meth. A 635 (1), 108-112 (2011).
[3] A. Singer et al., "Spatial and temporal coherence properties of single free-electron laser pulses," Opt. Express 20, 17480-17495 (2012).
[4] M. Bastiaans, "The Wigner distribution function applied to optical signals and systems," Opt. Commun. 25 (1), 26-30 (1978).
[5] B. Schäfer and K. Mann, "Characterization of an ArF excimer laser beam from measurements of the Wigner distribution function," New J. Phys. 13, 043013 (2010).
[6] C. Q. Tran et al., "Experimental Measurement of the Four-Dimensional Coherence Function for an Undulator X-Ray Source," Phys. Rev. Lett. 98, 224801 (2007).
[7] B. Schäfer et al., "FEL beam characterization from measurements of the Wigner distribution function," Nucl. Instr. and Meth. A 645, 502-507 (2011).
[8] M. J. Bastiaans, "The Wigner distribution function of partially coherent light," Opt. Acta 28, 1215-1224 (1981).
[9] M. J. Bastiaans, "Application of the Wigner distribution function to partially coherent light," J. Opt. Soc. Am. A 3, 1227-1238 (1986).
[10] B. Eppich et al., "Measurement of the four-dimensional Wigner distribution of paraxial light sources," Proc. SPIE 5962 (2005).
[11] ISO/DIS 11146-1 "Lasers and laser-related equipment – Test methods for laser beam widths, divergence angles and beam propagation ratios – Part 1: Stigmatic and simple astigmatic beams".

ISBN 978-3-95450-126-7

Table 2: Exemplary Results of First Measurements at the Extended Setup With Several Modes of an Nd:YAG Laser. Displayed distributions show radiation characteristics at the waist of the laser beam *before* the toroidal mirror, i.e. after leaving the resonator. Global degree of coherence is given as calculated value K and as theoretically expected value K_{th}.

	Projected Wigner distribution $h_x(x,u)$	Mutual coherence function $\Gamma(x,0,s_x,0)$	Near field $I(x,y)$	Global degree of coherence
TEM00	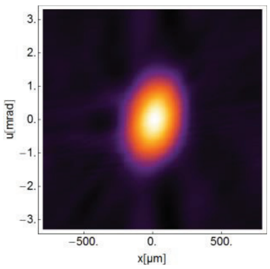	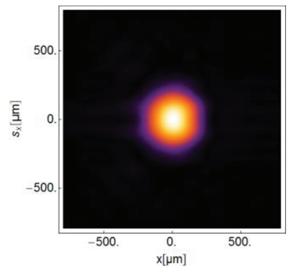	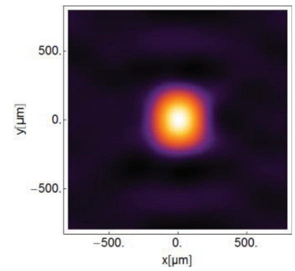	K = 0.99 (K_{th} = 1.00)
TEM11	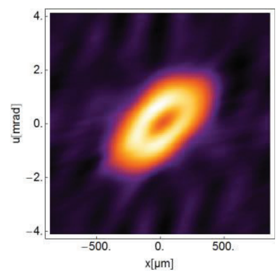	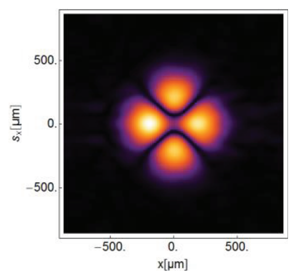	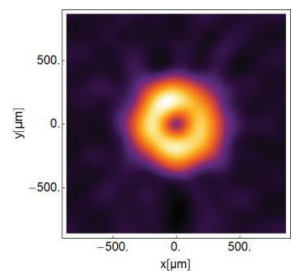	K = 0.46 (K_{th} = 0.50)
TEM20	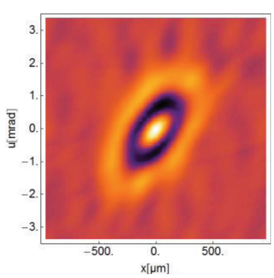	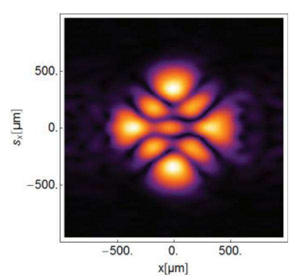	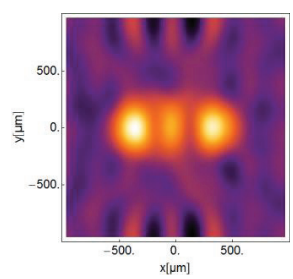	K = 0.96 (K_{th} = 1.00)

ISBN 978-3-95450-126-7